

Effects of climate and land use changes on runoff extremes

D. Pumo^{1*}, E. Arnone^{1,2}, A. Francipane¹, V. Noto¹ and G. La Loggia¹

¹ DICAM, Università degli Studi di Palermo, Italy

² Amigo climate s.r.l., Via Flaminia 48, I-00196, Roma, Italy

* e-mail: dario.pumo@unipa.it

Abstract: This work proposes a modeling framework for the analysis of alterations in the watershed hydrological response and, more specifically, in runoff extremes, induced by climate change and urbanization. A weather generator and a cellular automata land-use change model are used to generate hypothetical scenarios accounting for relevant trends at the global scale. Such scenarios are successively considered to force a spatial-distributed hydrological model, which simulates, at high time-resolution, most of the key hydrological variables at the basin scale. The framework is applied to the *Peatcheater Creek at Christie* basin (OK, USA). The considered climate alterations are negative and positive variations in mean annual precipitation, obtained by different configurations of rainfall intensity and frequency, and simultaneous increase in temperature. Urbanization is conceptualized by an increase in the fraction of impervious areas within the basin. The analysis of the hydrological response simulated under the different scenarios, shows how the considered perturbations, acting separately or combined, may significantly alter the runoff generation mechanisms, resulting in relevant alterations of the extreme runoff events intensity and their associated return period.

Key words: hydrological change, climate change, urbanization

1. INTRODUCTION

The alterations induced in many basins' hydrological processes by natural or anthropogenic perturbations are commonly referred to as "hydrological changes". The analysis of the hydrological changes and their interacting triggering factors are high-priority research objectives, also defined within the *Panta Rhei* decade 2013-2022. Climate change and urbanization are among the most recurrent causes for hydrological changes at the global level. While the former is surely one of the most studied causes in recent literature (e.g., Francipane et al., 2015; Pumo et al., 2016), the latter represents a potential driver for hydrological changes still rather unexplored (e.g., Pumo et al., 2017).

In this direction, this work aims to investigate possible alterations in the generation of basin scale runoff extremes due to these two types of perturbation acting singularly or in a combined manner. Specifically, we analyzed the peaks over threshold (POT) for the daily runoff and annual peaks of hourly runoff (HAP). Such indicators have been computed on the runoff time series for the river basin of the *Peatcheater Creek at Christie* (OK, USA), obtained by forcing a physically-based and spatial-distributed hydrological model by different hypothetical scenarios (combination of different synthetic climate schemes and land use maps).

2. METHODOLOGY

The proposed modeling framework involves the combined use of a land-use change model, a weather generator and a spatial-distributed hydrological model, briefly described below.

2.1 Land-use change model

We specifically developed a Land-Use Change Model (LUCM) with the aim to reproduce

possible future land-use maps which take into account the increase of urbanization. The model belongs to the class of probabilistic cellular automata models, based on: i) the consideration of the basin as a grid of regular cells; ii) the definition of an initial status (*urban* or *not-urban*) at any cell; iii) the iterative generation of a new grid at each successive temporal step according to time invariant fixed rules that determinate the new status in each cell as a function of its previous status and the status of the cells in its neighborhood. At each iteration, a value of probability of being urbanized (*urbanization probability*) is first associated to each *not-urban* cell and, successively, a new grid is generated starting from the previous one and replacing the cells with a higher *urbanization probability* by “new” *urban* cells.

The model considers an urban expansion criterion, according to which urban areas tend to expand around pre-existing urban zones following gentler slopes. The *urbanization probability* of each cell, in fact, depends on: 1) the slope (higher probability to cells with lower slope); 2) the total number of contiguous *urban* cells (i.e., within the Moore neighborhood, including the cells on a two-dimensional square lattice 3x3 around the analyzed cell); 3) the total number of *urban* cells in the neighborhood (i.e., within the extended Moore neighborhood, including the cells on a square lattice 7x7).

The model requires a raster map of slope and the initial status (*urban* or *not-urban*) of each cell within the basin. Model parameters are: the temporal horizon (generally equal to the simulation time of the application); the operative time step for new grids generation (e.g., 1 year); the projected future fraction of urban areas after the selected temporal horizon. A linear trend in built-up areas increase is assumed, so that urban expansion results constant year by year.

2.2 Weather generator and hydrological model

A weather generator is used to generate stationary climate schemes of current or possible future conditions. Specifically, we adopted the *Advanced WEather GENerator*, AWE-GEN (Fatichi et al., 2011), which is a statistical hourly stationary model capable to reproduce statistical properties of several weather variables (i.e., precipitation, cloudiness, radiation, temperature, and wind speed).

The adopted hydrological model is the *TIN-based Real-time Integrated Basin Simulator* - tRIBS (Ivanov et al., 2004a,b). It explicitly considers the spatial variability of land-surface descriptors and uses an adaptive multiple resolution approach, based on a triangulated irregular networks (TIN), to solve basin hydrology at very high temporal (i.e., hourly) and spatial (10-100m) resolutions, simulating most of the natural hydrological processes. Moreover, it simulates the interactions of the fluxes inside the surface soil layers (i.e., unsaturated zone and water table) and reproduces four different mechanisms of runoff generation.

3. CASE STUDY

A synthetic experiment is here carried out on the real case of *Peacheater Creek at Christie* (OK, USA), one of the basins originally used to calibrate and validate the tRIBS model. A 100m Digital Elevation Model (Fig. 1a), and information available from other previous works (e.g., Vivoni et al., 2004), have been retrieved and used to characterize the spatial distribution and the properties of soils and land cover, as well as the geomorphologic characteristics of the basin.

The basin's area is 64 km², with mean elevation of 328 m a.s.l. and slopes from 2% to 40%. The vegetation is a mixture of forest grasslands and cropland-urban areas with an impervious fraction estimated in about 1.6%. The predominant soil is made of gravelly silt loams. Precipitation and temperature are characterized by scarce seasonally, with mean annual values approximately equal to 1,160 mm/year and 14.6°C, respectively.

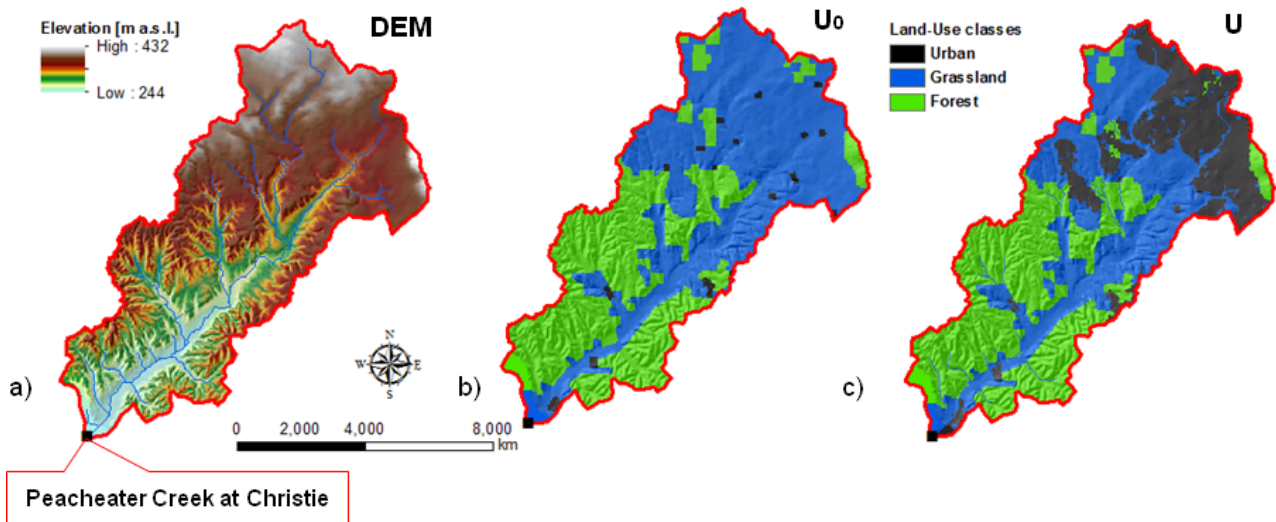


Figure 1. (a) DEM and stream network for Peacheater Creek at Christie, (b) Land Use Maps: observed current map U_0 and (c) Urbanized map (U) derived by the LUCM

3.1 Land use maps

The hydrological model is applied considering two different land use maps: the current map (U_0) and the altered map (U). In particular, U_0 (Fig. 1b) is the observed land use map and considers the same classification (i.e., *forest*, *grassland* and *urban*) and parameterization of Ivanov et al. (2004b).

The U map (Fig. 1c) is a possible future map obtained through the LUCM by increasing the fraction of impervious areas (replacing *not-urban* cells, previously classified as *forest* or *grassland*, with “new” *urban* cells). The working resolution is the same of the DEM (i.e., 100 m) from which the slope map has been derived. The used temporal horizon is equal to 100 years while the operative time step for new grids generation is equal to 1 year.

The urbanization process is highly variable in space and time and depends on a variety of local factors (e.g., socio-economic attractiveness, political, social, and geographical context, etc.). In view of the purposes of this work, we have imposed a percent increment of urban areas up to the 25% after 100 years, consistently with some trends observed in many fast developing regions of the world (e.g., Gumindoga et al., 2014).

3.2 Climate schemes and generation of different synthetic scenarios

Different, 30-year long, stationary climate schemes have been generated by using the AWE-GEN: the first is a reference period relative to the current conditions (*Baseline*), while the others represent possible future conditions obtained considering different climate change projections. The considered trends in the generation of each future climate scheme are not representative of projections specific for the area under analysis, but rather widespread limit conditions projected at the global level. In particular, climate changes considered for the generation of future climate schemes consist in relevant negative and positive trends in the Mean Annual Precipitation (MAP) and a simultaneous increase in temperature, according to some “highly probable” projections by the IPCC-5AR (IPCC, 2013). Other climate variables are assumed to maintain the observed statistical properties.

The *Baseline* has been created inferring the AWE-GEN climate parameters from hourly data recorded from 1992 to 1998 at the *Fayetteville* weather station (close to the basin: $36^{\circ}1'N$, $94^{\circ}16'W$).

Temperature time series for future climate schemes have been generated considering an increase (+2.6 °C) for the mean annual temperature. Two opposite limit conditions have been considered with regard to the generation of the precipitation time series for future schemes: a negative trend

(*CN*), consisting in a reduction by the 25% of the MAP, and a positive trend (*CP*), consisting in an increment by the 25% of the MAP. Four different types of climate scheme, characterized by different rainstorm characteristics, have been generated for both the *CN* and *CP* conditions:

- A. variation in MAP exclusively due to an equal percent variation in the frequency of rainstorms (-25% for CN_A and +25% for CP_A);
- B. variation in MAP entirely due to an equal percent variation in the mean intensity of rainstorms (-25% for CN_B and +25% for CP_B);
- C. variation in MAP resulting by the application of an equal percent variation to both the rainstorm frequency and intensity (i.e., -13.4% for the CN_C and +11.8% for the CP_C);
- D. variation in MAP due to an increase of the mean rainstorm intensity by the 50% for both the CN_D and CP_D and a consequent reduction of the frequency (-50% for CN_D and -16.67% for CP_D).

A total of 18 different stationary scenarios have been obtained by combining the 2 land use maps derived by the LUCM and the 9 climate schemes generated by the AWE-GEN. A code is here used to identify each scenario, with the first part referring to the climate scheme (*Baseline*, CN_i , or CP_i , with $i=A, B, C$, or D) and the second to the considered land use map (U_0 or U).

4. RESULTS

4.1 Analysis of the peaks over threshold

Peaks of daily runoff are analyzed in terms of mean annual percentage of days with runoff exceeding a fixed threshold (Peaks Over Threshold - POT). This last has been selected equal to the daily runoff value associated to the 90th percentile under the reference scenario (*Baseline*- U_0), i.e. the value that is currently exceeded for less than 36 days per year (i.e., 1.98 mm/day). The results are synthesized by the histogram in Fig. 1a, where the POT (% over the year) values are reported for each scenario; the variation with respect to the current value, expressed in terms of difference (Δ) in mean annual number of days with runoff over the selected threshold, is also reported by the label on the top of each bar.

Climate perturbation has a dominant role in determining hydrological changes, even if the role of land use change is not marginal, especially under the CN_i schemes. When only land use changes are considered (*Baseline*- U_2), the POT slightly increases.

When only negative climate trends are considered (scenarios with climate schemes CN_i and the U_0), the POT drastically reduces, with even 22 (i.e., CN_B) days per year less with runoff over threshold with respect to the reference scenario. Comparing the cases CN_B - U_0 and CN_D - U_0 it can be noticed that, at equal MAP, a higher POT is associated to the last case, whose mean rainstorms intensity is higher. When only positive climate trends are considered (scenarios with climate schemes CP_i), the POT significantly increases, with Δ ranging from 10 (i.e., CP_B and CP_D) to 19 (i.e., CP_A) days. The *CP* scheme associated to the scenario with the highest POT is that corresponding to the highest mean frequency and the lowest mean intensity of rainfall events (i.e., CP_A).

The combined application of climate and land use perturbations leads to contrasting effects on peaks generation, depending on the climate scheme considered. The effect due to the urbanization tends to smooth the reduction in the POT induced by the MAP reduction under the CN_i , especially for the climate scheme A, while it tends to exacerbate the increment in the POT caused by the MAP increment under the CP_i , especially for the scheme D. The only exception is the case under the CP_A , where POT and Δ are almost the same for both the U_0 and the U maps: in this case, an increment in the rainstorms frequency with unaltered intensity produces similar effects on daily runoff peaks considering both a fraction of impervious areas of the 1.6% and the 25%.

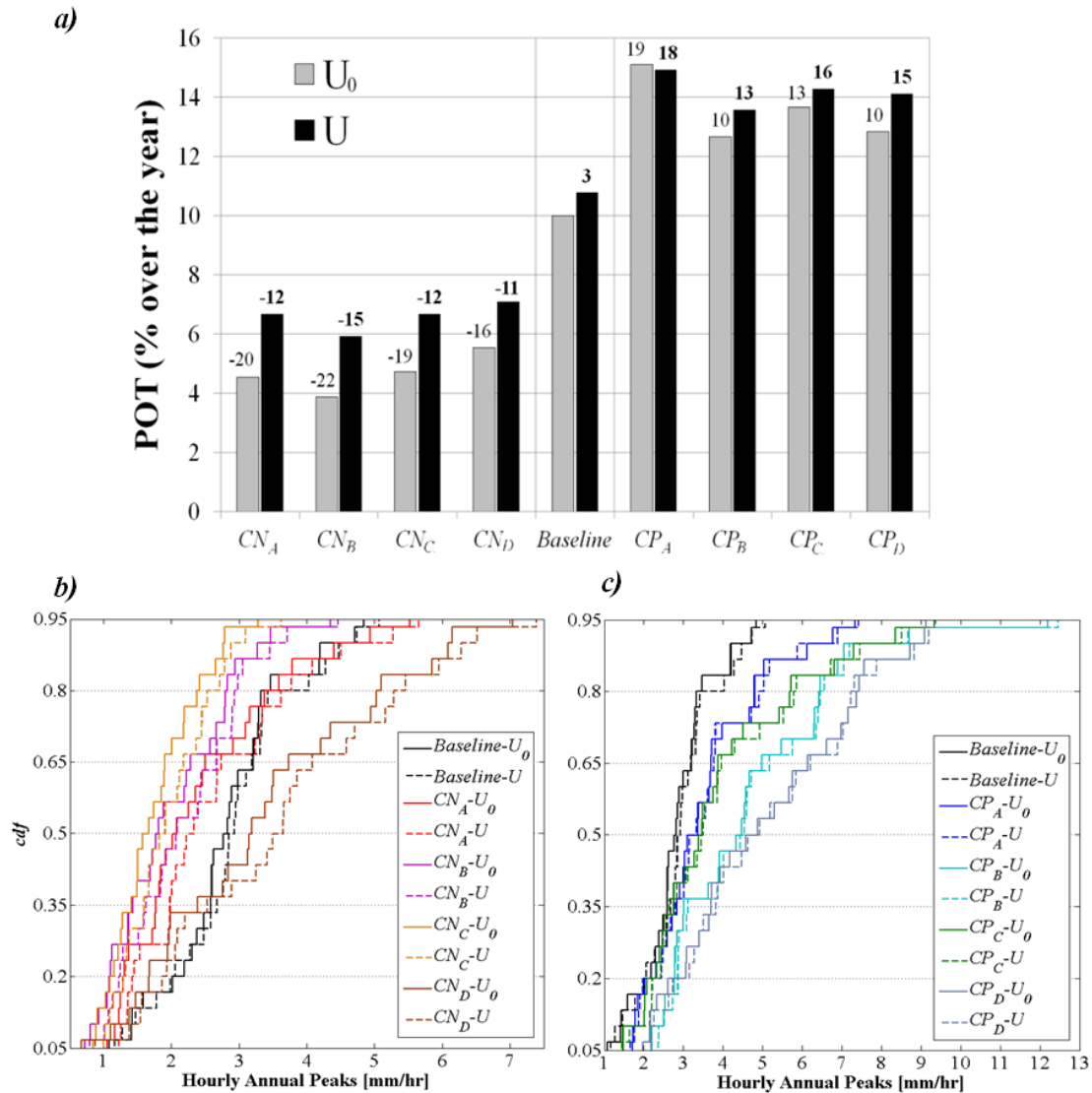


Figure 2. (a) Days per year with flow over threshold: POT (% over the year) reported by the histogram bars and variation Δ (days) with respect to the current scenario (labels). Cumulative distribution functions (cdf) of annual peaks of hourly runoff (HAP) derived from the hourly runoff time-series under the different scenarios considering the CN_i (b) and the CP_i (c) climate schemes

From our results it is then presumable that the POT is highly sensitive to rainfall intensity in conditions of limited MAP (e.g., CN scenarios), while, when MAP is higher (e.g., CP scenarios), rainfall frequency may have a predominant role in influencing the POT.

4.2 Analysis of the annual peaks of hourly runoff

Figure 2 also shows the cumulative distribution functions (cdf) of the Hourly Annual Peak (HAP) of runoff for each scenario. The upper and lower tails are not represented, focusing only on the probability domain from 5% to 95% and neglecting, then, possible outliers.

Under unaltered land use map, MAP reduction for the CN_i-U_0 scenarios (Fig. 2b) induces, except for the CN_D-U_0 , a drastic reduction of HAP especially for the more extreme values (upper tail of the cdf). For instance, under the CN_C-U_0 , both the mean and the median are reduced with respect to the $Baseline-U_0$ by about the 40%. Alterations induced by the CP_i-U_0 scenarios (Fig. 2c) result in higher HAP, with mean and median increased, on average, by the 56.6% and 39.2%, respectively. Under unaltered climate (i.e., $Baseline$), the urbanization process induces not negligible increments

in HAP values (mean and median increase by about the 3.6%).

The coupled application of climatic and land use changes implies a partial compensation of the effects on hourly runoff extremes for the case under climate schemes CN_i , while, in the case of positive trends in climate (under climate schemes CP_i), the effects of two perturbations are overlapping. It is worth emphasizing that the percent variations in HAP induced by the simultaneous application of the two perturbations are significantly different (lower in absolute value) from those resulting from the sums of the percent variation singularly induced by climate and land use changes.

Changes on HAP due to the consideration of a reduction in MAP with an increment in rainfall intensity (CN_D-U_0) are comparable to those induced by an increment in MAP through the only increment in rainfall frequency and unaltered rainfall intensity (CP_A-U_0). The two cases, characterized by markedly different values of MAP, exhibit similar HAP, with almost overlapping *cdfs*. When the U map is considered, the two cases (i.e., CN_D-U and CP_A-U) result even more similar with each other, with lower discrepancies for all the statistics.

Also with regard to the only other case under CN_i conditions where rainfall intensity is not reduced, i.e., the CN_A-U_0 , the upper part of the *cdf* (Fig. 2b) is basically unaltered with respect to the *Baseline-U₀*, demonstrating that changes in HAP, especially for what concerns the more extreme values, are highly sensitive to changes in rainstorm intensity rather than to changes in mean annual rainfall and, sometimes (as in the case CN_D-U_0), an increment in rainfall intensity could totally mask the effects on extreme hourly runoff due to a reduction in MAP.

The relevant sensitivity of hourly runoff peaks to rainfall intensity is also confirmed by the analysis of the cases under CP_i schemes; from Fig. 2c it is possible to observe how the raise in HAP is directly proportional to the trend magnitude applied to the rainstorm intensity. Simulations under the CP_D are, in fact, those showing the most severe variation in terms of HAP with respect to the *Baseline-U₀*, with a percent increment for the median of the *cdf* equal to 65.6% and 67.8% under the maps U_0 and U, respectively.

The analyzed perturbations have then a relevant impact on runoff extremes. For example, the extreme hourly runoff associated to the 90th percentile under the *Baseline-U₀* (i.e., about 4 mm/hr corresponding to a return period of 10 years) would be much more recurrent under the scenario CP_D-U (where it is characterized by a return period of only 2 years), while the HAP under the CP_D-U having a return period of 10 years would be more than two times (i.e., 9.2 mm/hr) the current value (Fig. 2c). Under scenarios considering CN_i schemes, the events with a return period of 10 years are reduced in magnitude for climate schemes with reduction in rainfall intensity (up to 2.7 mm/hr for the CN_B-U_0), it is almost unaltered for the schemes with unaltered rainfall intensity (CN_A) under both the U_0 and U, while it is significantly increased for climate schemes with increased rainfall intensity (up to 6.3 mm/hr for the CN_B-U). Thus, under drier annual precipitation conditions, extreme runoff events are particularly sensitive to the rainfall characterization, resulting increasing with rainstorm intensity, especially under more impervious land use conditions.

5. CONCLUSIONS

Climate changes and urbanization, acting separately or combined, may significantly alter the basin scale runoff generation mechanisms with evident modifications in runoff extremes. Our results have highlighted a strong not-linearity in the basin response to the change factors that makes the superposition principle scarcely applicable. With regard to the considered trends, climate changes have a clear predominant role in altering the main characteristics of runoff extremes. A careful characterization of rainstorm events seems to be a crucial aspect in such a kind of studies. Urbanization, whose effects results more evident when finer time-scales of analysis (i.e., hourly) are adopted, tends to smooth the effects due to the consideration of negative climate trends, while the opposite behaviour results under positive climate trends. Many of the evidences from this study can be explained looking at the modifications induced by the two perturbations here considered to the runoff components partitioning. Our simulation has shown how urbanization induced a major

production of the fastest component of runoff, the surface runoff for infiltration excess mechanism, and the same has been observed for climatic schemes with increased rainstorms intensity. An increased relative weight of such component with respect to the other implies an increase of the intensity of the runoff peaks.

REFERENCES

- IPCC Climate Change, 2013. The physical science basis. Contribution of Working Group I to the fifth assessment report of the Intergovernmental Panel on Climate Change. Cambridge University Press, Cambridge, United Kingdom and New York, NY, USA
- Ivanov, V.Y., Vivoni, E.R., Bras, R.L., Entekhabi, D., 2004a. Catchment hydrologic response with a fully-distributed triangulated irregular network model. *Water Resour. Res.*, 40(11), W11102
- Ivanov, V.Y., Vivoni, E.R., Bras, R.L., Entekhabi, D., 2004b. Preserving high-resolution surface and rainfall data in operational-scale basin hydrology: a fully-distributed physically-based approach. *J. Hydrol.*, 298 (1-4): 80-111
- Fatichi, S., Ivanov, V.Y., Caporali, E., 2011. Simulation of future climate scenarios with a weather generator. *Adv. Water Resour.*, 34(4): 448-467
- Francipane, A., Fatichi, S., Ivanov, V.Y., Noto L.V., 2015. Stochastic assessment of climate impacts on hydrology and geomorphology of semiarid headwater basins using a physically based model. *J. Geophys. Res. Earth Surf.*, 120: 507–533
- Gumindoga, W., Rientjes, T., Shekede, M.D., Rwasoke, D.T., Nhapi, I., Haile, A.T., 2014. Hydrological impacts of urbanization of two catchments in Harare, Zimbabwe. *Remote Sens.*, 6: 12544-12574
- Pumo, D., Arnone, E., Francipane, A., Caracciolo, D., Noto, L.V., 2017. Potential implications of climate change and urbanization on watershed hydrology, *Journal of Hydrology*, 554: 80-99, doi: 10.1016/j.jhydrol.2017.09.002
- Pumo, D., Caracciolo, D., Viola, F., Noto, L.V., 2016. Climate change effects on the hydrological regime of small non-perennial river basins. *Science of the Total Environment*, 542(Part A): 76-92
- Vivoni, E.R., Ivanov, V.Y., Bras, R.L., Entekhabi, D., 2005. On the effects of triangulated terrain resolution on distributed hydrologic model response. *Hydrological Processes*, 19(11): 2101–2122